Weener Igneous Complex: geochemistry and implications for the evolution of the Palaeoproterozoic Rehoboth basement inlier; Namibia

Thomas Becker[1], Brigitte Diedrichs[2], Bent T. Hansen[2] and Klaus Weber[2]
[1]Geological Survey, PO 2168, Windhoek, 9000, Namibia
e-mail: tom@mme.gov.na
[2]Institut für Geodynamik der Lithosphäre, Goldschmidtstr. 3, 37077 Göttingen, Germany

The Rehoboth Basement Inlier in the Southern Margin Zone of the Damara Orogen in Namibia comprises two main groups of volcanic and intrusive units: the ca. 1200 Ma Sinclair Sequence and the ca. 1800 Ma Rehoboth Sequence. Till recently, the evolution of the Rehoboth Sequence remained largely unknown. We present results of geochemical investigations carried out on the ca. 1765 Ma Weener Igneous Complex which represents a prominent igneous center in the Rehoboth Sequence. The WIC is a calc-alkaline gabbroic to granodioritic suite. Petrographic features from the other units of the Rehoboth Sequence and the so-called pre-Rehoboth basement are reviewed and support the emplacement of the older part of the Rehoboth Basement Inlier within an arc setting.

Introduction

The Rehoboth Basement Inlier (RBI) in the Southern Margin Zone of the Damara Orogen (Namibia) comprises igneous and sedimentary rocks (Fig. 1) that formed during Palaeoproterozoic and Mesoproterozic crustal growth. The tectonic setting and stratigraphy of Palaeoproterozoic (Ubendian-Eburnian) rocks are poorly understood. Contacts between individual formations are either tectonic and/or obscured by intrusions of which the Weener Igneous Complex (WIC) is a prominent representative. Being predominantly of intermediate composition, it is intrusive into and comagmatic with the metavolcanic rocks of the Gaub Valley Formation (Becker *et al.*, 1994). Meso-proterozoic volcano-sedimentary rocks of Kibaran age (1150-1250 Ma) are grouped into the Sinclair Sequence and coeval intrusives, interpreted to represent a major rift event (Borg, 1988). The aim of this study was two fold: (1) to give a detailed petrographic and geochemical description of the different rock types of the WIC and (2) to interpret the geotectonic setting of the Rehoboth Sequence within the framework of the Ubendian-Eburnean orogenic cycle.

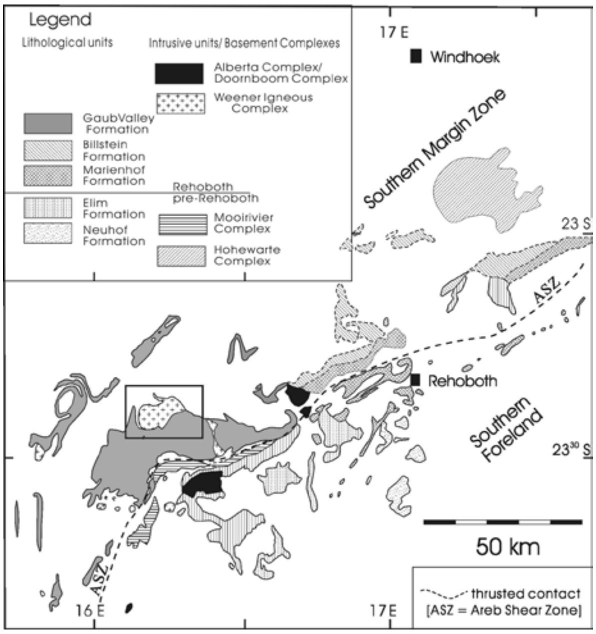

Figure 1: Areal extent of the Rehoboth Sequence and pre-Rehoboth units within the Southern Marginal Zone and the Southern Foreland of the Damara Orogen (study area shown by box).

Regional geology

The RBI is subdivided in Table 1 into (i) formations and high-grade metamorphic complexes of assumed pre-Rehoboth age (Neuhof and Elim Formations, Moorivier Complex), (ii) the *ca.* 1800 Ma Rehoboth Sequence (Marienhof, Billstein and Gaub Valley Formations), and (iii) intrusives temporally linked to the Rehoboth Sequence and show wide variation in composition (e.g. WIC, Piksteel Suite, Alberta and Doornboom Complexes). However, this stratigraphy is rather poorly constrained because most contacts between individual units are tectonic or obscured by subsequent intrusions. Distinction between pre-Rehoboth units and the Rehoboth Sequence itself is questionable because at present the pre-Damaran structural and metamorphic history is only poorly documented. Recent field work (Becker, in prep.) shows that (i) the Elim Formation transgresses the Gaub Valley Formation; and (ii) the Mooirivier Complex comprises rock types of the Gaub

Table 1: Stratigraphy proposed by Becker and Brandenburg (2000) based on new field evidence and geochronological data.

Stratigraphy		Intrusive units	Age	Method	Ref
Sinclair Sequence	Billstein Fm	Gamsberg Granite Suite	1099 ± 24	U/Pb zircon	3
Rehoboth Sequence		Piksteel Granite	1645 ± 41	U/Pb zircon	7
	Marienhof Fm				
		Alberta Complex Naub Diorite Weener Tonalite	1759±144 1725 ± 25 1765 ± 21	Sm/Nd wr Rb/Sr wr U/Pb zircon	8 2 5
	Elim Fm including Kamasis Member & Moorivier Member		1820 ± 144 1764 ± 56 1725 ± 10	Sm/Nd wr U/Pb sphene U/Pb zircon	4 8 4
	Gaub Valley Fm		1782 ± 10	U/Pb zircon	6
	Neuhof Fm		1784 ± 45	U/Pb zircon	1

References: **1**-Burger & Walraven (1978); **2**-Reid *et al.* (1988); **3**-Pfurr *et al.* (1991); **4**-Ziegler & Stoessel (1993); **5**-Becker *et al.* (1996); **6**-Nagel *et al.* (1996); **7**-Hilken (1998); **8**-Becker *et al.* (in prep)

Valley and Elim Formations that have been subjected to a higher metamorphic grade as a result of injection migmatisation rather than from a regional metamorphic event. In addition, age determinations on igneous rocks of both the pre-Rehoboth basement and the Rehoboth Sequence using the conventional U/Pb bulk zircon method yielded similar ages between 1860-1700 Ma, and suggest evolution of both units in only one major orogenic event (Becker, 1995; Becker, *et al.*, 1996; Nagel *et al.*, 1996).

The oldest unit of the sequence, the Neuhof Formation, comprises a bimodal volcanic succession and terrestrial sediments (Table 2). U/Pb zircon ages of supposedly Neuhof felsic volcanic rocks range from 1294 ± 25 Ma to 1784 ± 45 Ma (Burger and Walraven, 1978). Clearly, some supposed Neuhof acid volcanic rocks belong to the Sinclair Sequence. No contact has been reported with the Gaub Valley Formation to the north.

Conventional bulk zircon ages of the Gaub Valley Formation vary from 1747 +11 -8 Ma to 1794 +146 -75 Ma (Nagel *et al.*, 1996). Limnic-fluviatile metasediments predominate at the base of this unit; they interfinger with and are overlain by felsic tuffite. Geochemical results document affinity of these volcanic rocks with the WIC but they have a higher degree of differentiation (Becker, 1995). The contact to the overlying Elim

Table 2: Petrographic data of units of the Rehoboth Basement Inlier

Lithological unit	**Petrography** (after de Waal, 1966; Brewitz, 1974; Schulze-Hulbe, 1979; Schalk, 1988; Becker, 1995)
igneous rocks	- intruded by Gamsberg Granite Suite (of Sinclair age)
top	- lavas and sills: in few places intermediate to mafic (amygdaloidal) lavas or sills included in the Billstein F; usually altered to amphibolite;
	- schistose succession: mainly sericitic phyllite with intercalations of conglomerate and layers of grey quartzite; probably overlies sericite quartzite;
Billstein Formation	- sericite quartzite: hundreds of meters thick, from quartz-sericite schist to dense, sericitic quartzite often with cross-bedding and heavy-mineral bands up to 2 mm thick; bands or lenses of conglomerates intercalated in upper portion of unit; ubiquitous magnetite.
base	- basal conglomerate: pebbles from few cm to more than 20 cm (quartzite, granite, vein quartz, abundant fragments of sericite phyllite and rarely of mafic rocks); towards the east grades into gritty quartzite.
Areb Shear Zone	- prominant E-W striking shear belt; several phases of deformation. - later phase of intense shearing results in predominant transposition foliation and frequent zones of blastomylonite; these structures largely obliterate earliest phase of deformation. - earliest phase with tight to isoclinal folds plunging at varying angles from NW-SE to NNW-SSW; presumably pre-Damara.
Piksteel Suite	- granodioritic to granitic S- to I-type suite; $^{87}Sr/^{86}Sr$-initial 0.707 to 0.709; A/CNK values 1.0 to 1.4; at present ill defined and probably often confused with granitoids of Sinclair age; in general, only weakly deformed; intrusive into deformed rocks of the Rehoboth Sequence; ages vary from 1200 to 1780 Ma.
Alberta and Doornboom Complexes	- most prominent representatives of a series of mafic to ultramafic zoned and partly serpentinised bodies of hornblende gabbro from several meters to 16 km in size. - layered sequence of metagabbros intruded by a pegmatitic phase of similar composition as well as by pyroxenite, harzburgite and dunite. - outcrops form belt within the RBI with change in strike from N-S in the W (close to Solitaire) to W-E strike in the E. - some geochemical affinity to mafic volcanic rocks of the Elim Formation. - age poorly constrained at *ca.* 1442 Ma (Reid *et al.,* 1988) and ca. 1750 Ma (Becker, *et al.,* subm.).
igneous rocks	- intruded by Doornboom Complex.
	- mafic volcanics: abundant schistose mafic layers intercalated in sedimentary rocks, probably mafic to intermediate sills.
top	- conglomerate: of minor occurence and laterally not persistent; lenses and layers with grey quartzite, vein quartz, chert, rare granite and phyllitic fragments, interbedded with phyllite and quartzite.
	- pelitic rocks: mostly altered to fine-grained sericitic phyllite forming horizons up to several 100 m thick; very monotonous in appearance; locally bedding preserved; layers few mm to cm thick with gradation in grain size (slightly darker colour in lower portion).
Marienhof Formation	- sericite quartz phyllite: often grading into soft sericitic quartzite or locally into slate; thin layers of fine-grained quartzite < 1 m thick intercalated in thick phyllite horizons.
	- metaquartzite: grey to white, very dense; ranging in composition from pure quartzites (fine to medium grained, extremely dense, locally ripple-marks or cross-bedding preserved) to feldspathic or serictic varieties. However, probably not part of the Marienhof Formation but rather of the overlying Billstein Formation.
base	- felsic volcanics: at the base voluminous masses of quartz-feldspar porphyries (~1200 Ma); besides angular cognate clast fragments of sedimentary rocks (mainly quartzite); many intercalated layers of coarse pyroclasts. Felsic volcanics are probably part of Sinclair Sequence (1200 Ma).
igneous rocks	- intruded by Weener Igneous Complex, Alberta Complex, Naub diorite; minimum age *ca.* 1768 Ma.
	- ore deposits: several small occurences of Zn, Cu sulfides and Au (i.e Kobos, Samkubis, Moutonsvlei, Witkrans) ore deposits of probable submarine exhalative origin.
top	- volcanic rocks: several hundred meters intermediate to mafic lavas; primary structures often preserved (amygdales, flow-top breccias and scoriae); subordinate tuffites and felsic volcanic rocks.
	- marble: calcitic and dolomitic marble at various levels; combined thickness more than 400 m; often interfingers with calcareous schists; nodules of cherts and quartz encrustations ubiquitous.
Elim Fm	- mica schist: usually interbedded in successions of quartzite and mafic metalava; in some places rich in hematite pseudomorphs after pyrite.
	- magnetite quartzite (iron cherts): up to 1 m thick and partly with layering or lamination; associated iron-poor cherts.
base	- sericite quartzite: reddish to greyish sericite-rich quartzite dominates at the base of Elim F; primary structures (ripples, cross bedding) locally preserved; transition into mature quartzite and phyllite depending on sericite content.
igneous rocks	- intruded by Weener Igneous Complex, Alberta Complex, Piksteel Granite Suite; minimum age *ca.* 1782 Ma.
	- ferruginous quartzite: confined to highest level of sericite schist; transition into sericite schist and quartzite of Elim Fm.
top	- magnetite quartzite: very subordinate, in various stratigraphic positions.
	- sericite phyllite: finely laminated (metatuffites); locally chaotic volcanic deposits (conglomerate, breccia, lavas).
Gaub Valley Formation	- quartzite: hard, grey quartzite intercalated in sericite phyllite; rare cross-bedding preserved.
base	- conglomerate: more than 1000 m thick coarse conglomerate (quartzite, vein quartz, amphibolite, quartz porphyry, granite); intercalations of brown quartzite and micaceous quartzite; transition into monotonous succession of micaceous quartzite, and quartz sericite phyllite with intercalations of ferruginous quartzite; lenses of small pebble conglomerates comprise redeposited sericite phyllite.
igneous rocks	- intruded by Hammerstein granite (of unknown age) as well as Nubib granite (of Sinclair age).
Neuhof Formation	- layered succession of felsic and mafic volcanics, the latter mostly altered to amphibolites. - varying sediments such as fine-grained quartzites, conglomerates, phyllites and minor calcsilicates.

Formation, while mostly tectonised, seems to be gradational elsewhere and is marked by a transition from terrestrial to marine deposition, the latter predominating. Highly sheared mafic hyaloclastic volcanic rocks dominate at the top of the Elim Formation (Brewitz, 1974). They are intercalated with shallow marine sediments. One U/Pb sphene age of 1757 +67 -52 Ma has been determined on a rare interbedded felsic volcanic horizon (Becker *et al.*, in prep.). The final stage in basin evolution is marked by clastic sediments of the Marienhof Formation. Again, mafic volcanic rocks as well as intrusive sills are abundant, while calcareous rocks are missing.

The Marienhof and Elim Formations are cut by ultramafic to mafic intrusions that are partly layered. Geochemical data suggest a similar mantle source as for the volcanic rocks of the Elim Formation (Becker and Brandenburg, 2000). One Rb/Sr whole rock age of 1442 ± 32 Ma has been determined for the Alberta Complex (Reid *et al.*, 1988) which has a Sm/Nd whole rock age of 1750 ± 140 Ma (Becker *et al.*, in prep). All Palaeoproterozoic units were intruded by the Piksteel Suite of batholithic dimensions which varies in composition from granite through granodiorite to minor tonalite. U/Pb bulk zircon ages vary from 1057 ± 35 Ma to 1782 ± 8 Ma for supposed Piksteel rocks which again documents the difficulty of distinguishing similar looking Rehoboth and Sinclair granitoids. A syn- to post-collisonal origin of this magmatic suite has been proposed relative to deposition of the Rehoboth Sequence (Boehm, 1998). Finally, the youngest unit of the Rehoboth Sequence is the Billstein Formation. It comprises a fining-upward sequence of clastic rocks, with conglomerates and gritty quartzites grading upwards into schistose sericite quartzite. In contrast to the underlying formations, deformation and metamorphic grade are relatively low and intrusions are of Mesoproterozoic age only.

Weener Igneous Complex

The WIC is a *ca.* 110 km^2 elliptical complex containing a great diversity of fine- to medium-grained orthogneisses. Composition ranges from tonalite and granodiorite in the centre through gabbro and granodiorite in the marginal zone. Microgranite forms a ring dyke (Fig. 2). Various types of mafic enclaves occur throughout the central body. These are amphibole/biotite-rich enclaves, and rounded, magmatic amphibole/plagioclase enclaves up to several decimetres in size. Mafic and felsic angular fragments up to 5 m across occur mainly close to the margin of the complex and are clearly xenoliths from underlying country rock. The WIC is intrusive into the surrounding volcanic rocks of the Gaub Valley Formation which are thought to be coeval with the WIC (Becker *et al.*, 1994). The WIC is intruded by

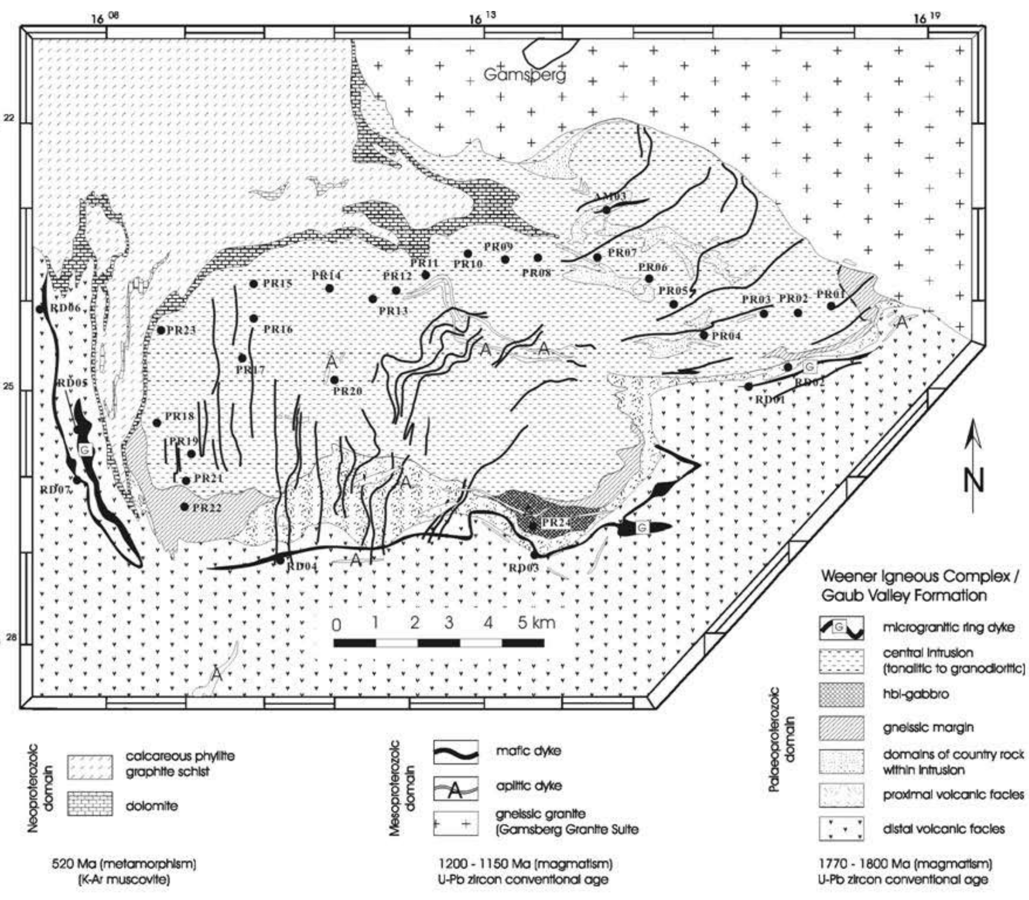

Figure 2: Simplified geological map of the study area showing location of samples.

the younger Gamsberg granite.

The magmatic texture of the WIC has been overprinted by at least three metamorphic events which have blurred primary structures: (i) Pre-Sinclair metamorphism is documented by xenoliths of gneissic WIC in the Gamsberg granite; (ii) contact metamorphism in the vicinity of the Gamsberg granite is shown by a zone of hornblende hornfels several metres wide which indicates intrusion of the granite at a shallow crustal level; (iii) regional-scale overprint of greenschist to lower amphibolite facies metamorphism during the Damara orogeny which produced a ramifying gneissic refoliation.

The main components of WIC rocks are plagioclase (unzoned oligoclase with local retrograde alteration rims of albite), quartz, biotite, varying amounts of amphibole (Ca-Mg hornblende to tschermakite), as well as secondary epidote and chlorite (Table 3). Accessory phases comprise zircon, sphene, apatite, magnetite and secondary muscovite and garnet. Modal proportions of the main intrusive phases suggest classification as hornblende gabbro, tonalite and trondhjemite for the central body and granite for the ring dyke.

Conventional U/Pb bulk zircon analyses yielded ages between 1743 +87 -61 and 1767 +53 -24 Ma for the WIC (Becker, *et al.*, 1996). Gaub Valley Formation ages range between 1747 +11 -8 and 1794 +146 -75 Ma (Nagel *et al.*, 1996).

Geochemical characteristics of the WIC have been based on few whole rock analyses (de Waal 1966; Stoessel and Ziegler, 1988; Ziegler and Stoessel, 1993). A/CNK ratios above 1.1, together with low Rb, Nb and Y contents, suggest that the WIC granitoids originated from the melting of a sedimentary source rock during a collisional event. However, this is in conflict with low initial $^{87}Sr/^{86}Sr$ values reported by Seifert (1986) and Reid *et al.* (1988).

Geochemistry

Sampling

Samples (PR01-PR23) with *ca.* 500 m sample spacing were taken roughly along the long axis of the WIC (Fig. 2). Additional samples stem from the gabbroic margin (PR24), ring dyke (RD01-RD07), ultramafic pyroxenites (now amphibolite) in stocks and dykes (AM03) and amphibolitic (XE01, XE02, XE04) and amphibole/biotite-rich enclaves (XE03, XE05) of the central intrusion.

Analytical methods

Samples were powdered with the aid of a jaw crusher and an agate mill. Major and trace elements (Table 4) were determined using a Philips PW 1400 sequential X-ray fluorescence spectrometer and ARL 72000 quantometer (Institute of Mineralogy, Göttingen). Analytical errors are below 1% for major elements and below 5% relative for trace elements. Detection limits are 5 ppm for Sc, V, Co, Cr, Zn, Rb, Ga, Sr, Y and Nb, and 10 ppm for Ni, Zr, Ba, Pb and Ce. Concentrations of Nb are close to the detection limit and, hence, subject to high analytical uncertainties. H_2O+ was determined by the Karl-Fischer method. Twelve samples were analysed for REE, U and Th using an ICP-MS (Table 5). Prepara-

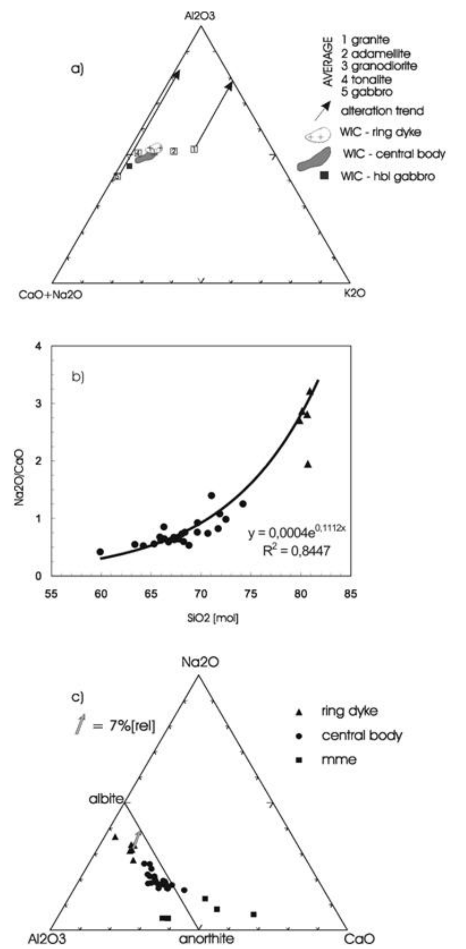

Figure 3: Assessment of alteration: a) Comparison of data set with fresh plutonic rocks (Nesbitt and Young, 1984); b) presentation of rocks samples in the Na_2O/CaO vs. SiO_2 [mol] diagram, and c) in a ternary CaO-Na_2O-Al_2O_3 [mol] diagram showing the mixing line between albite and anorthite.

Table 3: Mineral composition of samples of the Weener Igneous Complex (data from Groote-Biedlingmeier, 1974; de Waal, 1966; Becker, 1995).

	CA17	CA 31	CA 47	CA 50	WN 8	SAW 524	SAW 524A	PR24	PR127	PR13
quartz	25	15.9	14.1	24.5	28.6	24.1	32.6	14.3	25.7	22.5
plagioclase	39.8	46.1	34.7	36.4	37.2	55.4	33.4	23.2	35.9	38.4
biotite	14.1	21.6	19.6	19.7	15.6	10.1	27	9.5	16.5	19.3
epidote	8.2	11.7	8.0	9.4	14.5	2.4	2.7	6.3	6.0	9.5
albite	2.3	1.6	5.5	0.6	2.4					1.3
amphibole	8.7	-	-	3.4		6.8	2.8	42.6	6.6	6.3
chlorite	1.4	2.3	-	5.4	-			0.75	8.3	0.5
garnet	-	0.1	1.5	-	-					
apatite	0.2	0.8	1.2	0.1	0.1					
ore minerals	0.9	0.2		1.0	0.5	1.2	1.5	2.9	1.1	1.2

tion of the solutions followed Heinrichs and Hermann (1990). International standards (Ja-2, Jb-3) were analysed at the same time as the samples and are compared with accepted values.

Assessment of alteration

Lower amphibolite facies metamorphism of the WIC is likely to have mobilised H_2O and CO_2 as well as alkali and alkaline-earth elements. H_2O values below 2.5 wt.% (Table 4) probably indicate limited hydration. Petrographic observations document limited element transport of soda and calcium by saussuritisation of plagioclase. Binary diagrams show considerable scatter not only of alkalis but of all elements around inferred linear or curved trends.

However, straight liquid lines of descent are unlikely to occur within the WIC since cumulate formation, assimilation of country rock, mixing of different magma sources and autometasomatism are likely to obscur simple fractionation trends. Bivariate diagrams of alkalis vs. immobile incompatible elements (i.e. Zr, Nb) are even less applicable within granitoids because these elements are concentrated in accessory phases with uneven distribution. However, several points argue against extensive exchange of mobile elements during metamorphism. (1) All samples plot in fields of unweathered rocks (Fig. 3a). This is supported by CIA values ranging from 45 to 55 (Table 4) which are typical for fresh rocks of tonalitic to granitic composition. (2) Limited transport of soda and calcium is suggested by the steady increase of these elements as well as the Na_2O/CaO ratio with increasing SiO_2. This most likely results from primary fractionation processes (Figs. 3b and 9) as major element transport would have obscured such trends. Samples clearly define a magmatic trend with early separation of Ca-rich plagioclase and hornblende (enclaves and hornblende gabbro) followed by fractionation of Na-rich plagioclase as well as biotite in tonalitic rocks and, in addition, by muscovite in granitic rocks of the ring dyke (Fig. 3c). Accordingly, early, Ca-rich, fractionated rocks gradually changing into more evolved rocks with higher aluminium and soda content. (3) Rb/Sr whole rock and U/Pb bulk zircon ages yielded similar results (1650 Ma vs. 1750 Ma) for the WIC, and document only limited alteration of rubidium and strontium. Accordingly, the alteration present in the WIC is not considered to be sufficiently intense to preclude the employment of geochemical classification methods on these rocks. In contrast, considerable element transport took place within mafic magmatic enclaves and is documented by a high scatter of most elements.

Major elements

The main intrusion of the WIC is characterised by SiO_2 values between 58-68 wt.% with a bimodal distribution (e.g. 60-62 and 66-68 wt.%). Rocks with dis-

Table 4: Chemical composition of samples of the WIC. Determined by XRF.

Sample	PR01	PR02	PR03	PR04	PR05	PR06	PR07	PR08	PR09	PR10	PR11	PR12	PR13	PR14	PR15	PR16	PR17	PR18
Latitude	23 24 02	23 24 05	23 24 05	23 24 20	23 24 02	23 23 50	23 23 35	23 23 35	23 32 35	23 23 30	23 23 45	23 23 55	23 24 00	23 23 55	23 23 53	23 24 12	23 24 45	23 25 20
Longitude	16 17 40	16 17 10	16 16 45	16 15 50	16 15 27	16 15 10	16 14 30	16 13 45	16 13 18	16 12 50	16 12 10	16 11 50	16 11 25	16 10 55	16 09 50	16 09 53	16 09 45	16 08 35
SiO2	60.5	60.1	60.6	62.6	63.1	63.5	61.1	60.6	61.6	59.7	59.5	61.7	64.2	66.4	62.8	67.8	61.4	66.8
TiO2	0.81	0.90	0.90	0.78	0.65	0.80	0.85	0.90	0.79	0.85	0.90	0.77	0.81	0.55	0.99	0.57	0.94	0.64
Al2O3	15.7	16.1	16.1	15.6	14.8	14.7	14.8	16.2	16.0	15.7	16.2	15.6	15.0	15.0	14.8	14.5	15.8	15.9
Fe2O3	6.72	7.73	7.62	6.66	5.50	5.80	6.21	7.47	6.78	7.33	8.00	6.75	6	5.05	7.79	4.83	7.58	4.27
MnO	0.09	0.12	0.14	0.11	0.11	0.08	0.08	0.12	0.10	0.12	0.14	0.11	0.09	0.09	0.16	0.08	0.12	0.06
MgO	2.53	2.99	2.95	2.59	2.00	2.04	2.23	3.09	3.19	3.35	3.17	3.33	2.32	2.58	2.81	1.85	2.73	1.26
CaO	4.41	5.22	5.26	4.50	3.33	3.54	3.49	4.82	3.97	5.54	5.38	4.87	3.85	2.79	4.07	3.15	4.87	3.97
Na2O	2.88	3.21	3.10	3.14	3.40	2.90	2.93	3.60	3.74	3.35	3.11	3.33	3.24	4.31	3.02	3.43	3.47	3.61
K2O	2.02	1.99	1.95	2.42	2.48	2.22	2.41	1.92	2.22	1.61	2.03	2.10	2.79	2.06	2.72	2.52	1.96	2.14
P2O5	0.26	0.20	0.20	0.18	0.13	0.03	0.03	0.29	0.16	0.17	0.21	0.16	0.14	0.17	0.19	0.11	0.21	0.14
H2O+	1.50	1.28	n.a	1.40	1.40	1.13	1.51	1.10	1.37	1.95	1.48	1.38	1.1	1.03	1.42	1.13	1.27	1.14
Sum	97.42	99.84	98.82	99.98	96.89	96.73	95.64	100.11	99.93	99.67	100.12	100.10	99.54	100.03	100.77	99.97	100.34	99.93
CIA	51.2	48.8	49.0	49.4	50.8	51.9	51.8	49.1	50.4	47.5	48.7	48.4	49.4	51.0	49.2	50.7	48.6	50.7
Rb	76	71	82	96	87	77	80	63	68	47	81	65	87	60	97	67	74	53
Zr	183	204	201	180	165	242	224	216	205	196	200	173	229	153	248	163	207	231
Y	17	27	45	27	24	7	7	37	31	34	51	33	38	15	39	22	38	17
Nb	6	7	9	9	9	6	9	8	9	5	9	8	8	6	10	5	14	5
Sr	320	312	322	288	275	298	294	357	314	358	313	339	313	285	291	285	320	297
Pb	6	16	18	19	13	12	12	14	8	8	15	8	13	11	13	11	15	15
Ga	15	17	21	15	16	15	16	16	15	17	16	16	15	14	17	16	17	15
Zn	75	76	127	65	61	61	67	69	69	69	84	69	63	62	85	50	75	45
Ni	38	44	50	42	29	30	33	46	50	70	52	69	30	32	37	28	31	12
Co	21	26	24	23	15	18	19	24	20	28	24	25	18	15	21	16	23	13
Cr	57	56	59	51	38	49	50	52	62	80	63	90	42	59	55	39	53	22
V	106	117	116	113	90	97	91	127	112	121	123	113	93	81	120	77	125	69
Ba	953	694	710	477	827	898	963	844	901	873	639	800	1005	731	987	1180	523	1535
Sc	17	9	25	16	6	14	14	25	24	14	25	19	19	5	16	13	18	10

Sample	PR19	PR20	PR21	PR22	PR23	PR24	RD01	RD02	RD03	RD05	RD06	RD07	AM03	XE01	XE02	XE03	XE04	XE05
Latitude	23 25 47	23 24 57	23 26 05	23 26 25	23 24 20	23 26 45	23 25 00	23 24 50	23 27 03	23 25 30	23 24 10	23 24 30	23 23 02					
Longitude	16 09 10	16 11 00	16 09 00	16 09 00	16 08 40	16 13 40	16 16 25	16 17 05	16 13 50	16 07 45	16 07 10	16 07 20	16 14 35					
SiO2	61.6	66.3	60.9	66.4	59.9	51.8	75.2	76.2	77.5	76.2	76.1	76.3	46.9	49.5	48.4	55.2	49.4	59.3
TiO2	1.00	0.74	0.94	0.76	0.99	1.46	0.13	0.19	0.02	0.12	0.10	0.13	0.64	1.22	1.18	1.04	1.19	0.93
Al2O3	15.3	15.0	15.7	15.1	16.1	17.0	13.1	12.5	13.2	13.0	12.9	12.9	7.5	14.9	11.9	12.3	8.3	13.4
Fe2O3	7.32	5.22	6.71	5.54	7.95	12.6	2.38	2.31	1.36	2.37	2.21	2.39	12.6	11.1	12.5	12	13.7	11.44
MnO	0.12	0.09	0.10	0.07	0.13	0.18	0.05	0.04	0.07	0.04	0.03	0.04	0.20	0.17	0.23	0.26	0.27	0.25
MgO	2.44	1.48	1.97	1.73	3.19	4.43	0.29	0.29	0.02	0.25	0.24	0.15	18.3	8.74	12.1	5.4	13.6	5.09
CaO	4.54	3.41	4.07	3.19	5	7.46	1.49	1.68	0.44	1.51	1.33	1.39	9.34	9.08	8.6	4.3	10.5	4.37
Na2O	3.22	4.07	3.29	4.42	3.3	3.44	4.45	3.61	4.91	4.78	4.72	4.31	0.76	2.7	1.52	0.6	1.09	0.636
K2O	2.38	2.38	2.23	1.8	1.8	1.13	1.35	2.34	1.72	1.25	1.93	1.83	0.18	0.17	1.16	4.9	0.2	4.423
P2O5	0.2	0.21	0.19	0.14	0.2	0.13	0.09	0.05	0	0.07	0.02	0.02	0.18	0.1	0.15	0.2	0.06	0.197
H2O+	1.04	0.93	1.2	n.a	n.a	n.a	0.89	0.77	0.77	0.83	0.55	0.79	3.01	1.29	2.85	2.3	1.77	1.62
Sum	99.16	99.83	97.30	99.15	98.56	99.58	99.41	99.98	100.02	100.42	100.13	100.25	99.57	98.91	100.57	98.89	100.00	101.63
CIA	48.7	49.2	50.8	50.1	49.4	45.4	53.3	52.0	55.1	52.1	51.2	52.7	28.9	41.3	38.1	46.4	28.3	49.2
Rb	76	91	83	67	54	44	38	63	58	40	50	57	1	2	38	175	3	160
Zr	215	224	281	232	210	114	114	138	70	108	98	108	86	89	162	141	122	87
Y	29	37	34	38	26	29	21	30	32	22	28	28	16	30	45	138	110	91
Nb	7	9	13	11	8	4	9	9	7	10	11	10	3	6	12	17	14	13
Sr	304	263	289	306	353	282	178	209	91	175	245	188	99	142	146	195	32	231
Pb	12	15	11	12	7	8	11	19	12	12	21	14	6	0	0	4	0	9
Ga	19	14	17	16	18	20	13	13	15	14	13	14	11	16	19	17	15	21
Zn	79	57	77	48	75	203	32	39	34	26	27	39	97	75	125	163	132	144
Ni	26	10	17	13	38	48	0	0	0	1	0	0	856	156	403	82	461	37
Co	25	14	18	14	26	40	4	8	3	3	5	2	91	48	57	32	58	29
Cr	39	18	30	22	55	24	7	7	4	8	6	5	1187	407	776	193	951	242
V	111	76	92	78	129	243	13	13	7	12	10	9	124	253	208	145	206	132
Ba	1053	691	952	1054	564	479	837	887	1487	767	918	899	92	14	317	1277	67	1154
Sc	17	9	16	11	22	26	7	9	5	6	9	2	25	41	40	67	76	88

Table 5: ICP-MS analyse of selected samples of the WIC. Comparison of our analyses of international standards (JA2, JB3) with values given by Govindaraju, 1995; relative errors are calculated using the averages of our values and those of Govindaraju, 1995.

	PR01	**PR10**	**PR14**	**PR18**	**PR20**	**PR24**	**RD03**	**RD07**	**AM03**	**XE01**	**XE02**	**XE03**	**XE05**
Sc	14.4	17.1	11.0	8.7	14.9	25.6	4.77	6.53	24.2	39.7	37.0	75.9	77.7
Rb	82	53	60	54	89	39	52	57	2	1	37	2	174
Sr	205	345	287	301	258	275	88	189	94	144	149	28	198
Nb	11.9	11.7	9.7	8.8	16.6	7.3	12.5	15.7	4.16	1.78	7.5	10.8	18.8
Cd	0.03	0.07	0.01	0.01	0.06	0.07	0.03	0.03	0.05	0.10	0.13	0.22	0.34
Cs	2.42	0.94	3.42	0.92	1.44	1.24	0.21	0.58	0.00	0.00	0.98	0.00	3.54
Ba	914	807	703	1449	649	473	1377	881	77	22	324	49	1202
La	12.6	27.6	16.6	23.9	35.2	13.1	11.5	36.3	14.2	3.23	17.6	18.1	43.5
Ce	32.5	57.7	39.7	46.9	70.3	28.8	32.3	81.8	36.9	7.71	50.0	63	106
Pr	3.30	7.53	4.01	5.69	8.92	4.00	3.91	10.1	4.82	1.64	7.7	11.4	17.7
Nd	14.0	30.6	15.2	22.2	35.6	18.1	16.6	39.9	21.6	9.16	34.9	59.2	79.9
Sm	3.33	6.7	3.01	4.14	7.61	4.62	4.93	8.4	5.03	3.27	8.85	18.6	21.3
Eu	1.50	1.51	0.87	1.86	1.64	1.44	0.97	1.77	1.31	1.07	1.92	2.30	2.47
Gd	3.35	6.0	2.93	3.84	6.7	4.81	4.67	6.5	4.27	4.23	9.5	19.9	26.3
Tb	0.49	0.90	0.41	0.49	1.02	0.77	0.82	0.92	0.58	0.70	1.23	2.98	2.92
Dy	2.90	5.41	2.43	2.76	6.14	4.84	5.55	5.14	3.06	4.80	7.87	19.4	19.8
Ho	0.57	1.08	0.48	0.53	1.23	0.99	1.19	0.98	0.54	1.05	1.61	3.90	4.13
Er	1.55	3.08	1.39	1.48	3.60	2.81	3.65	2.78	1.46	3.10	4.67	10.8	11.7
Tm	0.22	0.45	0.22	0.21	0.55	0.42	0.60	0.40	0.20	0.45	0.68	1.53	1.59
Yb	1.36	2.86	1.35	1.29	3.56	2.63	4.06	2.65	1.27	2.88	4.38	9.3	9.8
Lu	0.20	0.41	0.19	0.20	0.53	0.40	0.61	0.39	0.19	0.42	0.64	1.29	1.38
Hf	0.41	0.84	1.90	0.80	1.55	1.04	3.06	3.16	1.88	0.42	1.42	1.86	0.39
Ta	1.47	1.89	2.46	1.50	3.23	1.73	3.68	3.72	1.90	1.03	3.11	4.36	13.1
Pb	9.5	8.8	9.4	11.12	12.1	8.3	9.0	12.3	3.51	4.79	3.64	1.79	9.5
Th	5.5	6.2	4.84	6.0	8.3	4.28	9.2	14.3	2.23	0.09	1.78	1.26	4.08
U	0.56	0.87	0.77	0.84	1.84	0.58	1.36	1.67	0.67	0.07	0.48	0.33	0.66
	JA-2*	**JA-2***	JA-2	JA-2	JA-2	relative error [%]		**JB-3***	**JB-3***	JB-3	JB-3	relative error [%]	
Sc	**19.25**	**19.60**	18.25	16.81	16.90	-10.84		**35.81**	**33.80**	33.63	33.38	-3.73	
Rb	**72**	**73**	71	67	67	-6.04		**14**	**15**	15	15	2	
Sr	**259**	**248**	250	234	246	-4.00		**419**	**403**	379	398	-6	
Nb	**10.00**	**9.47**	4.22	3.67	2.56	-64.2		**2.00**	**2.47**	2.75	2.84	25.02	
Cs	**4.83**	**4.63**	5.17	4.94	4.71	4.50		**0.90**	**0.94**	0.85	0.86	-7.13	
Ba	**281**	**321**	321	309	309	4.07		**245**	**245**	236	236	-4	
La	**16.48**	**15.80**	16.96	16.62	16.66	3.75		**8.28**	**8.81**	8.62	8.64	1.00	
Ce	**35.09**	**32.70**	35.04	34.38	33.95	1.66		**20.94**	**21.50**	21.98	22.17	4.03	
Sm	**3.32**	**3.11**	3.52	3.48	3.46	8.49		**4.36**	**4.27**	4.76	4.73	9.93	
Eu	**0.87**	**0.93**	0.96	0.94	0.91	4.03		**1.25**	**1.32**	1.34	1.33	3.78	
Tb	**0.51**	**0.44**	0.50	0.50	0.42	-0.09		**0.66**	**0.73**	0.73	0.74	6.06	
Yb	**1.80**	**1.62**	1.74	1.76	1.79	3.04		**2.63**	**2.55**	2.49	2.49	-3.90	
Lu	**0.33**	**0.27**	0.26	0.27	0.27	-10.61		**0.40**	**0.39**	0.37	0.38	-4.63	
Hf	**2.80**	**2.86**	2.88	2.91	2.78	0.86		**2.66**	**2.67**	2.62	2.66	-1.02	
Ta	**0.88**	**0.80**	2.50	2.51	1.27	198		**0.15**	**0.15**	2.27	2.28	1417	
Th	**5.43**	**5.03**	5.55	5.81	5.65	8.43		**1.28**	**1.27**	1.37	1.34	6.30	
U	**2.08**	**2.21**	2.23	2.43	2.20	6.66		**0.39**	**0.48**	0.44	0.49	6.72	

*Values given by Govindavaju, 1995.

tinctly lower SiO_2 occur in the marginal zone of the WIC (sample PR24), whereas the highest SiO_2 contents (75-78%) was found in rocks of the ring dyke.

The main WIC body comprises dominantly tonalite and granodiorite, whereas the ring dyke is granitic (Fig. 4). A/CNK values of 0.83-1.08 [mol] and A/NK values of 1.6-2.4 (Fig. 5) classify the samples as metaluminous to slightly peraluminous (Shand, 1951). A tendency is evident of increasing A/CNK and decreasing A/NK ratios with increasing SiO_2. Biotite and hornblende are suggested as primary phases in the AB diagram (Debon and LeFort, 1983). K_2O/Na_2O-ratios [wt.] are consistently below one with Na_2O concentrations above 3 wt.%. The rocks are calc-alkaline (Fig. 6). Together with low initial $^{87}Sr/^{86}Sr$ values (Seifert, 1986; Becker *et al.*, 1997) this classifies the WIC as an I- or M-type granitoid (Chappell and White, 1974). The samples plot in the gabbro, tonalite and granodiorite fields of DeLaRoche *et al.* (1980) (Fig. 7). They define a variation trend typical of that of subduction generated magmas (Batchelor and Bowden, 1984). Comparison of the WIC with geochemical characteristics (alkali-calc index, Shand's index, Na_2O/CaO, Na_2O,K_2O, MgO/FeO, MgO/MnO, A/NK) from granitoids of different tectonic

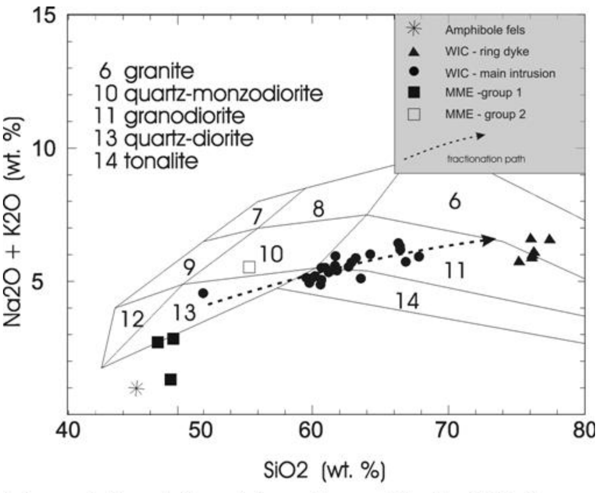

Figure 4: Presentation of the analyses within the TAS diagram (LeMaitre *et al.*, 1989).

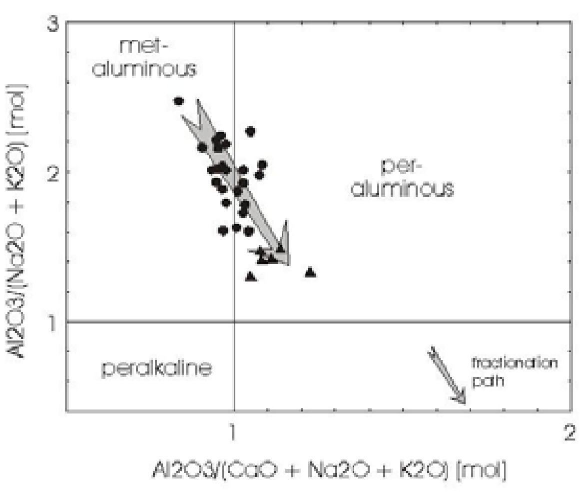

Figure 5: Presentation of the analyses within the A/NK vs. A/CNK diagram (Shand, 1951). Symbols as in Fig. 4.

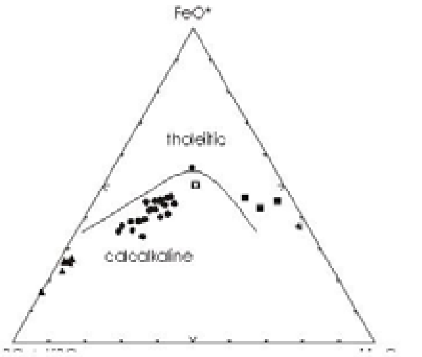

Figure 6: Presentation of the analyses within the ternary AFM diagram [FeO* = FeOtot] (Kuno, 1968). Symbols as in Fig. 4.

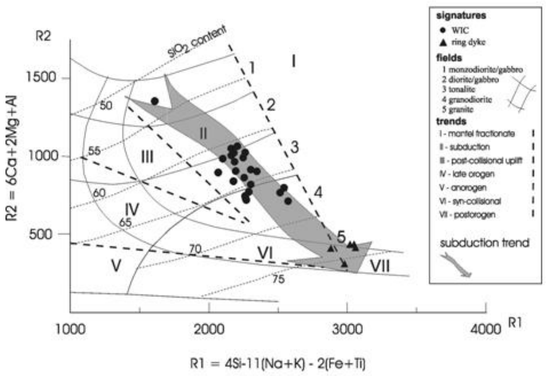

Figure 7: Presentation of the analyses within the R1-R2 classification diagram (DeLaRoche *et al.*, 1980).

typical for island arc or N-MORB basalts. However, modification of the enclaves by the surrounding magma most likely took place and casts doubt on the applicability of classification diagrams in this case. The second group (XE03, XE05) is characterised by the highest potassium (up to 5 wt.%), higher SiO_2 (up to 59 wt.%) and much lower Mg and Ca concentrations (5 and 4 wt.%).

The composition of the ring dyke is very homogeneous and plots on the trend defined by other rocks from the WIC (Fig. 9). SiO_2 increase is associated with concomitant decrease of TiO_2, Al_2O_3, Fe_2O_3, CaO, MgO and MnO, as well as with an increase of K_2O and Na_2O. P scatters widely, with a tendency to decreasing values with higher silica.

Mafic enclaves show a much wider range in element distribution than rocks from the central intrusion. Group I samples as well as the pyroxenitic rock (AM03) plot either on a linear continuation of the other samples (Fe_2O_3, MnO, CaO) or define segmented trends (TiO_2, Al_2O_3, MgO, Na_2O, K_2O, P_2O_5). Group II samples in general plot off these trends.

settings (Maniar and Picolli, 1989) suggests development within a volcanic arc setting.

The mafic magmatic enclaves (MME) have a great geochemical diversity (Tables 4 and 5) and can be divided into two groups. Samples XE01, XE02 and XE04 (Group I) have low alkalis, high magnesia (8.7-13.6 wt.%) and SiO_2 values around 50 wt.%, which classifies them as tholeiitic basalts (Figs. 4 and 6). These samples plot in the island arc tholeiite field (Fig. 8). In a variety of classification diagrams, the first group plots in fields

Trace elements

K-group (Ba, Sr, Rb)

Negative correlation with SiO_2 is evident only for Sr and documents the diadochous exchange of Sr by Ca, while Rb and Ba replace K (Fig. 10). The ratios of K/Rb and K/Ba of 197-335 and 12-42, respectively, are typical for calc-alkaline granitoids.

HFSE-group (Zr, Nb, Y)

Zr, Nb and Y show no obvious trend with increasing SiO_2 content although there is a suggestion of a negative correlation between Zr and SiO_2 and a positive one between Nb and SiO_2. Low Rb, Nb and Y contents (Fig. 11) classify the WIC rocks as volcanic arc granites (Pearce *et al.*, 1984).

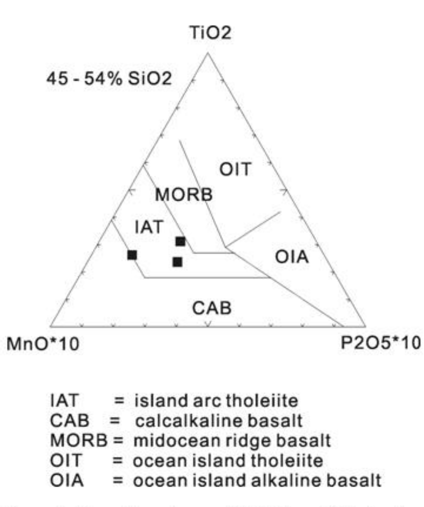

Figure 8: Presentation of analyses of MMEs within the ternary Ti, Mn, P diagram (after Mullen, 1983).

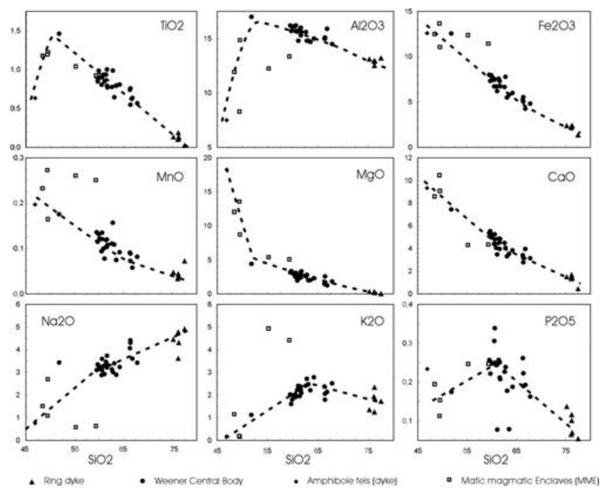

Figure 9: Presentation of the analyses in Harker diagrams (major elements). Inferred trends are indicated by stippled lines.

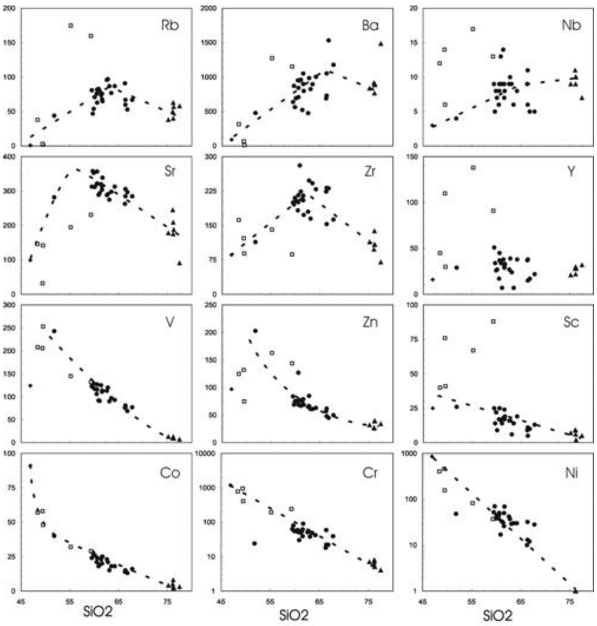

Figure 10: Presentation of the analyses in Harker diagrams (trace elements). Inferred trends are indicated by stippled lines. Symbols as in Fig. 9.

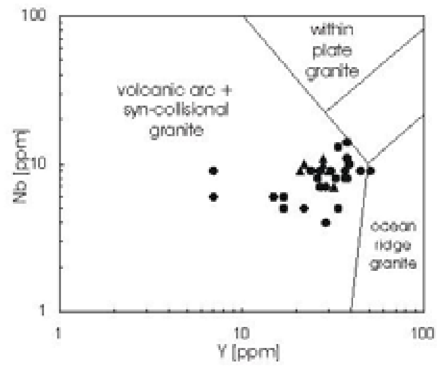

Figure 11: Presentation of the analyses within the Nb vs. Y tectonic classification diagram (Pearce *et al.*, 1984).

Transition and compatible elements (Ni, Co, Cr, V, Sc, Zn)

These elements decrease strongly with increasing SiO_2 which is attributed to the diadochous replacement by Mg and/or Fe. In comparison with modern calc-alkaline magmatic rocks, concentrations of compatible group elements are significantly higher which is in good agreement with data from Ziegler and Stoessel (1993). The range of Zn concentrations (40-90 ppm) is similar to values found in modern calc-alkaline suites (Brown *et al.*, 1984).

Normalised Trace Element Patterns

Rare Earth Elements

The ranges of chondrite-normalised REE patterns are: ∑REE = 87-198 ppm; $[La/Lu]_N$ = 1.93-12.51, and Eu/Eu* = 0.60-1.40 (Fig. 12). There is no correlation between the Eu anomaly of the rocks and their SiO_2, CaO and ∑REE contents. Three groups can be distinguished. The first group shows the lowest content of LREE $[La/Lu]_N$ = 1.93 and no Eu anomaly (sample PR24). The ∑REE (88 ppm) is within the range of the second group (see below), while ∑HREE (18 ppm) is comparable to the third group. The second group shows the lowest concentrations of both ∑HREE [9-12 ppm] and ∑REE [78-95 ppm] and a slight negative to significant positive Eu anomaly [0.84-1.40] (samples AM03, PR01, PR14, PR18). A positive correlation occurs between SiO_2 content and ∑REE (except for AM03). The $[La/Lu]_N$ ratios [6.5-12.5] are similar to those of the other groups. The third group displays higher ∑HREE [20-23 ppm] and ∑REE [151-198 ppm] as well as a significant negative Eu/Eu* ratio [0.69-0.71] (PR10, PR20, RD07). SiO_2 does not correlate with ∑REE. The first and third groups are from the margin and the second group is from the centre of the WIC (Fig. 2).

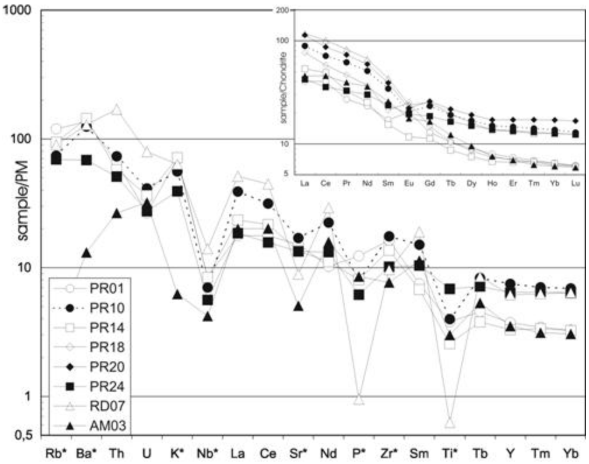

Figure 12: PM-normalised TE pattern of rocks from the WIC, (* = analysed by XRF-technique, other by ICP-MS). The inset shows chondrite-normalised REE abundances of the respective samples.

REE analyses of the MME are presented in Figure 13 together with the compositional range of the WIC, average N-MORB and average amphibole. Sample XE01 is characterised by a trend nearly parallel to the x-axis, with a slight depletion of LREE and no Eu/Eu*. The other enclaves are progressively enriched in REE and exhibit marked negative Eu anomalies. Initial increase of LREE is followed by convex arrangement in more altered samples. Here, patterns are dominated by those of amphibole separates.

Multi-element plots

The primitive mantle (PM)-normalised trace element pattern (Fig. 12) shows that increase from the more compatible to the incompatible elements (right to left) is common to all samples of the WIC (except AM03). The highest ratios occur within the group of hydrophile elements (Rb, Ba, Th, U and K). Ratios of Ti, P, Sr and Nb are lower than those of neighbouring elements forming negative spikes. However, these spikes are less pronounced within the least evolved rock (sample PR24).

Comparison of the U, K, Nb, Zr and Ti distribution with calc-alkali magmatic rocks from Meso- to Cenozoic granitoids (Fig. 14) suggests evolution of the WIC within a primitive continental or island volcanic arc (Brown *et al.*, 1984). According to these authors, depletion of Ba, Sr, P and Ti in granitoids of mature volcanic arcs results from higher fractionation of alkali feldspar, plagioclase, apatite and Fe-Ti oxides. Increase in Rb, Th, U, Nb and Y probably reflects AFC processes which become more important with increasing crustal thickness.

Marked differences between MME samples are also revealed by the PM-normalised spidergram (Fig. 13). While sample XE01 approximates N-MORB composition, the other samples show a general increase of ratios

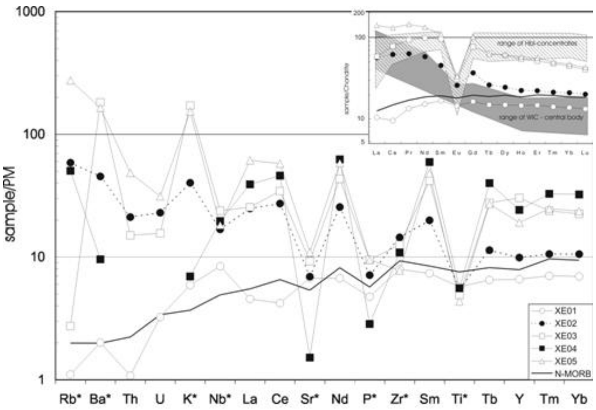

Figure 13: PM-normalised TE pattern of mafic magmatic enclaves. Inset shows chondrite-normalised REE abundances. Range of WIC as well as of amphibole concentrate have been plotted for comparison.

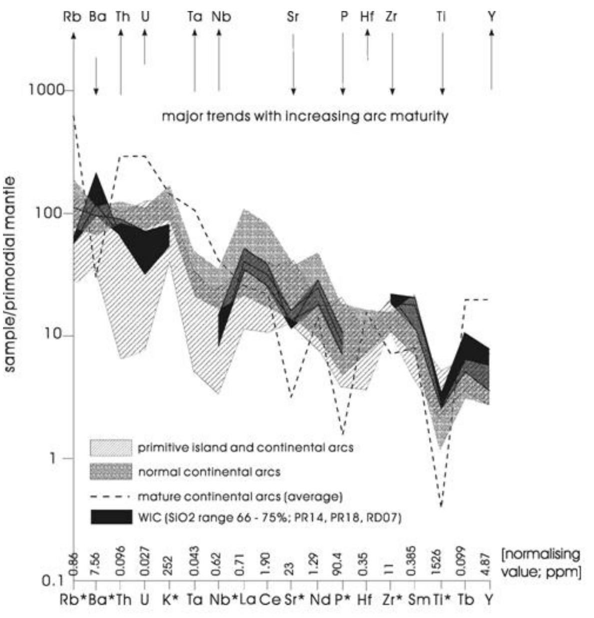

Figure 14: Comparison of mantle-normalised element pattern from the WIC (PR14, PR18, RD07) with modern granitoids from Mesozoic and Cenozoic magmatic arcs (compiled by Brown *et al.,* 1984).

from right to left, with marked negative spikes for Ti, P, Sr and Nb. Negative spikes of Zr, P, Th and U occur in the K-rich enclaves. Negative anomalies increase with the inferred degree of MME assimilation by the surrounding magma.

Isotope systematics

Whole rock analysis of Rb/Sr and Sm/Nd has been carried out on samples covering the compositional range of the WIC. The isotopic composition of Nd and Sr has been recalculated at 1800 Ma, the approximate emplacement age of the WIC. For comparison, typical N-MORB has been included in Figure 15. WIC samples form a curved trajectory that is typical of rocks formed by binary mixing of two homogeneous end members. Decrease of ε_{Nd} and increase of ε_{Sr} is evident with the inferred degree of fractionation from sample PR24 to RD07. In contrast, sample XE01 plots far off this trend, the off-set being caused by an extremely high ε_{Sr} value, while ε_{Nd} lies between values of sample PR24 and N-MORB.

Discussion and conclusions

Petrogenesis of the WIC

Main intrusion and ring dyke

Evolution of the magmas that form the WIC granitoids are constrained by the following:

(1) Geochemical patterns document multiple magmatic processes within source magma chambers: Immobile incompatible and rare earth elements of the parental magma are probably best approximated by amphibolite which occurs as dykes and pIUGS within the main intrusion (AM03). Gabbroic rocks (sample PR24) are present in the marginal zone and represent an amphibole-clinopyroxene rich cumulate, whereas rocks from the main intrusion vary from tonalitic to granodioritic in composition. At a still later stage, highly fractionated granitic magmas (RD01-RD07) were emplaced within a ring dyke.

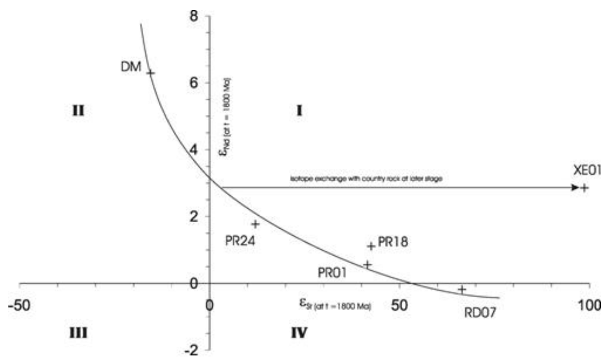

Figure 15: Presentation of Sr-Nd whole rock isotope systematics. Epsilon values have been recalculated at t = 1800 Ma which is considered as the approximate emplacement age for the WIC.

This sequence of crystallisation is partly reflected in bivariate element diagrams (Figs. 9 and 10). Compatible elements (Al, Fe, Mn, Mg, Ca, V, Zn, Sc, Co, Cr, Ni) decrease with the inferred degree of fractionation. However, elements which are incompatible in basaltic magmas display segmented trends (except Ti and Na): In most diagrams increase in concentration occurs from amphibolite through gabbroic to tonalitic rocks (SiO_2 <65 wt.%), whereas in more differentiated rocks concentrations either remain constant (Ba, Nb, Y) or decrease (K, P, Rb, Sr, Zr).

Such element behaviour is best explained by combined crystallisation of Ca-plagioclase, hornblende, magnetite, biotite, zircon, apatite and sphene. These minerals are part of the modal paragenesis and are probably igneous in origin. Elements which are incompatible within a basaltic magma during ascent become compatible with one or more mineral phases within a shallow magma chamber. Accordingly, highly fractionated rocks from the ring dyke are depleted in most elements.

(2) Further insight into shallow magma chamber processes as well as source characteristics is given by variation of REE. (i) The REE pattern of the amphibolite (sample AM03) lacks an Eu anomaly and shows limited LREE enrichment. This suggests a mantle source for the parental magma and only minor crustal contamination. Depending on the degree of partial melting, both depleted and enriched mantle could evoke such a pattern. (ii) The early magma composition is represented by rocks from the margin of the WIC. Crystallisation of hornblende produced a decrease of LREE/HREE in cumulate gabbro and increase of this ratio within the melt. However, since gabbroic rocks are rare compared to the central intrusion the latter effect has been insignificant. (iii) Crystallisation of Ca-plagioclase prevailed during the main stage and is documented by plagioclase cumulates with positive Eu anomalies (samples PR14, PR18). (iv) Within the remaining melt this resulted in a negative Eu anomaly (samples PR10, PR20 and RD07). However, there is no correlation between silica content and ∑REE of samples from stage (iii) and (iv). In addition, Eu peaks of both stages intersect each other. These features may result from only low proportions of trapped melt (hosting the REE) in more evolved rocks.

(3) Most elements scatter around the inferred line of liquid descent. This may be caused by various factors such as (i) increased incorporation of elements into minor and accessory minerals during crystallisation (Zr, P, Ti, Nb, Y, Sc), (ii) cumulate and assimilation processes (major oxides, Ni, Cr, Co), (iii) some post-magmatic alteration (Ba, Rb, K, Na), and (iv) analytical uncertainties (Nb, Y, P).

(4) Sr and Nd isotope systematics (at 1800 Ma) suggest mixing of an upper crustal component and a depleted mantle magma. Thereby, crustal contamination increases with the inferred degree of fractionation (as a function of silica) and is highest in the granitic ring dyke.

(5) Classification diagrams which are mostly based on alkaline and earth-alkaline elements probably are of limited use. However, assessment of alteration obviously shows limited element mobility only and, hence, allows cautious application of such diagrams. In general, they show that granitoids of the WIC are calc-alkaline and metaluminous to peraluminous. Low HFSE, Nb, Y and Rb contents as well as low initial $^{87}Sr/^{86}Sr$ values suggest emplacement within a volcanic arc.

(6) Pronounced negative Nb and Ti anomalies in combination with relatively high Ba, Zr, Ti and low U and Hf contents suggest an origin of the magma within a primitive magmatic arc (Brown *et al.*, 1984). The distribution of mantle-derived elements typical for marginal basins and mid-ocean ridges requires only a small to moderate degree of mantle melting (Pearce and Parkinson, 1993). A less pronounced Ti anomaly of cumulate hornblende gabbro (sample PR24) is likely to result from predominant crystallisation of hornblende, magnetite and sphene, opposing source characteristics. Early precipitation of these phases augments negative spikes in more fractionated magma, whereas significant P and Sr anomalies are related to fractionation of apatite and plagioclase.

Mafic Magmatic Enclaves (MMEs)

The abundance of MMEs is characteristic for calc-alkaline granitoids of active continental margins and island arcs (Didier, 1973). Their origin is, however, still the subject of much debate (Barbarin *et al.*, 1989, Dorais *et al.*, 1990) and they are thought to represent either (i) restite from anatectic melt processes, (ii) incorporated and modified mafic country rock, (iii) recycled early fractionate from the wall or floor of the magma chamber, (iv) mafic cumulate, or (v) blobs/pillows of inmiscible mafic liquid within a felsic host.

(1) Analysis of the MMEs document their great diversity which may result from different origins, magma mixing, and finally, varying degree of assimilation and element exchange during interdiffusion processes.

(2) High affinity of sample XE01 with N-MORB composition is evident from REE and incompatible and compatible element distribution (Figs. 9, 10, 13 and 16). In contrast to the WIC, no enrichment of LIL elements is observed. This might argue for interpretation of XE01 being a xenolith and indicate that the underlying country rock is partly composed of N-MORB. Such juxtaposition of tholeiitic and calk-alkaline rock suites has been reported from the New Hebrides back arc (Maillet *et al.*, 1995). However, high ε_{Sr} (at 1800 Ma) shows that isotopic equilibration with country rock occured at some post-magmatic stage and probably also affecting distribution of mobile elements.

(3) Mixing combined with crystal fractionation is suggested by several binary plots where amphibolitic enclaves lie along hyperbolic branches of segmented element trends (i.e. Co, Cr, Ni, Ti, Al, Mg, Ca). In the ε_{Nd} vs ε_{Sr} diagram (Fig. 15), projection of sample XE01

is possible on a mixing curve between depleted mantle and an upper crustal source. Samples from the WIC are aligned along this curve but have a higher proportion of crustal contaminant.

(4) Diffusion during the magmatic stage is believed to account for the different compositions of amphibolite and alkali-rich biotite/amphibole enclaves. Depending on the involved mineral reactions: (i) Fe, Mg, Ca and H_2O may be introduced into or removed from the enclaves; (ii) Si, Al and the alkalis diffuse invariably into the enclaves, and (iii) HFSE (e.g. Ti, Zr) are almost immobile and therefore can be used as reference components (Cramer and Kwak, 1988). Assuming a common source for all enclaves, the exotic composition of samples XE03 and XE05 may be explained by one of these processes.

(5) Finally, progressive assimilation of between 8 - 81% of the enclaves by the surrounding magma may be considered as important for the gradual change in REE distribution of the enclaves provided that all enclaves have the same origin (Tindle, 1991).

In summary, a complex magmatic and post-magmatic history for the analysed enclaves is evident with several processes operating on individual specimens in varying degrees. Unfortunately, the limited data set does not definitely preclude the enclaves being interpreted as modified country rock or as blobs of immiscible mafic magma. Hence, analysis of large mafic angular xenoliths close to the contact is required to favour one of these hypotheses. Diffusion processes as well as assimilation best explain variation in elements of more modified enclaves.

Geotectonic setting

Petrogenesis of the WIC suggests a subduction-related environment at *ca.* 1800 Ma. Deposition of sediments and volcanics in such a setting is possible within (i) the trench, (ii) the fore-arc basin within the arc-trench gap, (iii) small intra-arc basins within the magmatic arc and (iv) the back-arc (Fig. 16a, after Dickinson, 1973). Lithological sequences within these regions are characterised by calc-alkaline volcaniclastic deposits, highly variable sediments within the back arc (as a function of relief and downwarping rate) and by calc-alkaline volcanic rocks within the arc. Hence, contemporaneous supracrustal successions from the Rehoboth Sequence should exhibit similar characteristics with respect to style of sedimentation, magmatism, and metamorphism.

Deposition of the Rehoboth Sequence took place within a terrestrial to shallow marine environment (Table 2). Geochemistry of the coeval WIC indicates proximity to a volcanic arc at about 1800 to 1700 Ma. A remnant basin situation is inferred towards the end of the Eburnean-Ubendian orogeny because at 1.8 Ga, deformation and metamorphism of this orogenic belt was already completed (Fig. 16b). Preservation of terrestrial

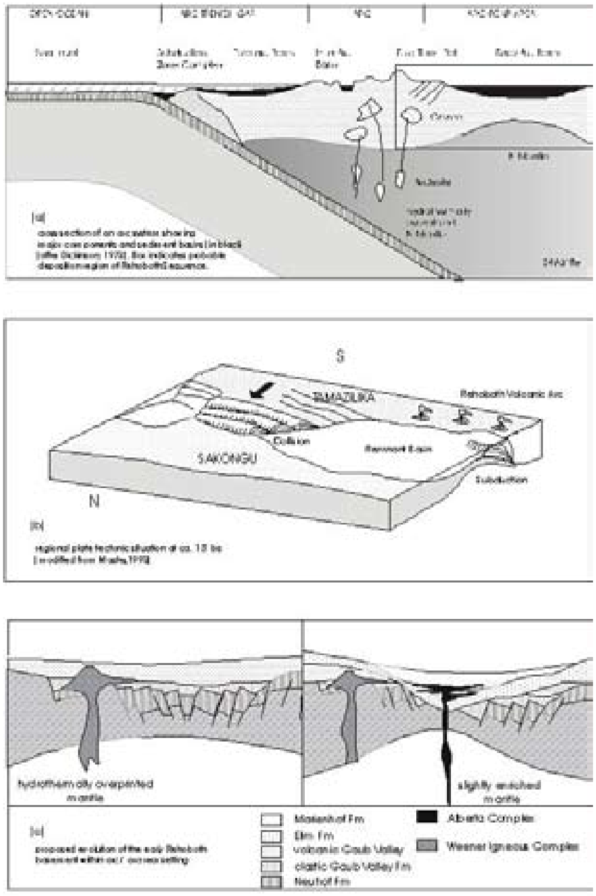

Figure 16: Model for the evolution of the Rehoboth Sequence within an arc/back-arc setting.

to shallow marine sediments, low-grade metamorphism and weak deformation suggest a back-arc rather than an arc or fore-arc setting (Fig 16c). Basal coarse clastics of the Gaub Valley Formation, preservation of volcanics and/or volcanic-derived sediments with arc signature, and the geochemical characteristics of the WIC, document priximity to an active magmatic arc. Further lithospheric stretching resulted in crustal down-warping and change from terrestrial to shallow marine deposition (Elim Formation). High proportions of mafic volcanic rocks and volcanic-derived sediments clearly are evidence for attenuated crust. Geochemical patterns of these mafic volcanics document decreasing influence of any arc (Becker and Brandenburg, 2000). Deposition of the Marienhof Formation may have taken place during further subsidence of the basin. Dominance of graded metapelites and shale interbedded with arenite, quartzite and scarce conglomerates may represent a slope facies. Large portions of mafic schist from this unit are probably volcanic in origin. However, recent field work shows that parts of the supposed Marienhof Formation actually belong in the Sinclair Sequence which hampers any interpretation. Subsequently, mafic to ultramafic bodies, which include the Alberta and Doornboom Complexes, intruded the Rehoboth Sequence. The close association of the Alberta Complex with mafic volcanics of the Elim Formation suggests a similar magma source for these two units. Eburnean magmatism terminated with the emplacement of the Piksteel Granitoid Suite. Again, geochronological data from different outcrops show that both Eburnian and Kibaran granitoids have been included in this unit. Therefore, the extent and importance of the Eburnian domain remains unknown. Finally, the Billstein Formation may either have been deposited during the molasse stage of the Eburnean-Ubendian event or it has no genetic relationship to this orogeny at all.

On a regional scale, geochronological and geochemical data show that the Rehoboth Sequence probably forms the southwestern continuation of the Eburnean-Ubendian Orogen. Crustal segments of similar age extend from equatorial Africa through southern Africa to southern Brazil and constitute a major crust-forming event (Masters, 1990).

Acknowledgements

This work was funded by the research grant AZ.1166/5.1 of the Deutsche Forschungsgemeinschaft (DFG) and carried out in collaboration with the Geological Survey of Namibia. F.Warkus and F.Oelsner kindly corrected a first version. H.Porada, H.Kampunzu, D. Reid and U.Schreiber are thanked for helpful comments and suggestions.

References

Barbarin, B., Dodge, F.C.W., Kistler, R.W. and Bateman, P.C. 1989. Mafic inclusions, aggregates and dikes in granitoid rocks, central Sierra Nevada Batholith, California, analytical data. *Bull. U.S. geol. Surv.*, 79 pp.

Batchelor R.A. and Bowden, P. 1984. Petrogenetic interpretation of granitoid rock series using multicationic parameters. *Chem. Geol.*, **48**, 43-55.

Becker, T. 1995. *Die Geologie, Geochemie und Geochronologie des Weener Igneous Komplex und der Gaub Valley Formation in der the Südlichen Randzone des Damara Orogens, Namibia und ihre Bedeutung für die Entwicklung der frühproterozoischen Rehoboth Sequenz*. Cuvillier, Göttingen, 250 pp.

Becker, T. and Brandenburg, A. (2000). The evolution of Alberta Complex, Naub Diorite and Elim Formation within the Rehoboth Basement Inlier/Namibia, geochemical constraints. *Communs geol. Surv. Namibia*, **12** (this volume).

Becker, T., Ahrendt, H. and Weber, K. 1994. The geological history of the Pre-Damaran Gaub Valley Formation and Weener Igneous Complex in the vicinity of Gamsberg. *Communs geol. Surv. Namibia*, **9**, 79-91.

Becker, T. Hansen, B.T., Weber, K. and Wiegand, B. 1996. U-Pb and Rb-Sr isotopic data of the Mooirivier Complex, the Weener Igneous Suite and the Gaub Valley Formation (Rehoboth Sequence), Nauchas area and their significance for the Paleoproterozoic evolution of Namibia. *Communs geol. Surv. Namibia*, **11**, 31-46.

Becker, T., Wiegand, B., Hansen, B.T. and Weber, K. Submitted. Isotope systematics (Sm/Nd, Rb/Sr, U/Pb) of the Elim Formation, the Alberta Complex, and the Weener Igneous Complex - probable genetic links between Palaeoproterozoic magmatic rocks of the Rehoboth Basement Inlier: Namibia. *Communs geol. Surv. Namibia*.

Boehm, A. 1998. *Geochemische Untersuchungen an basischen und felsischen prae-damarischen Gesteinen am Suedrand des Damara Orogens (Farm Areb), Namibia*. Unpubl. Diplom thesis, Univ. Goettingen, 62 pp.

Borg, G. 1988. The Koras-Sinclair-Ghanzi rift in southern Africa: Volcanism, sedimentation, age relationships and geophysical signature of a late middle Proterozoic rift system. *Precambr. Res.*, **38**, 75-90.

Brewitz, H.W. 1974. Montangeologische Erkundung und Genese der metamorphen, exhalativ-sedimentären Zn-Cu-Lagerstätte Kobos im Altkristallin des Nauchas Hochlandes, SW-Afrika. *Clausthaler Geol. Abh.*, **18**, 128 pp.

Brown, G.C., Thorpe, R.S. and Webb, P.C. 1984. The geochemical characteristics of granitoids in contrasting arcs and comments on magma sources. *J. geol. Soc. London*, **141**, 413-426.

Burger, A.J. and Walraven, F. 1978. Summary of age determinations carried out in the period April 1974 to March 1975. *Ann. geol. Surv. S. Afr.*, **11**, 317-322.

Chappell, B.W. and White, A.J.R. 1974. Two contrasting granite types. *Pacific Geol.*, **8**, 173-174.

Cramer J.J and Kwak, T.A.P. 1988. A geochemical study of zoned inclusions in granitic rocks. *Am. J. Sci.*, **288**, 827-871.

Debon, F. and Le Fort, P. 1983. A cationic classification of common plutonic rocks and their magmatic associations: principles, method, applications. *Bull. Mineral.*, **111**, 493-510.

DeLaRoche, H., Leterrier, J., Grandchaude, P. and Marchal M. 1980. A classification of volcanic and plutonic rocks using R1-R2 diagram and major element analyses - its relationships with current nomenclature. *Chem. Geol.*, **29**, 183-210.

De Waal, S.A. 1966. *The Alberta Complex, a metamorphosed layered intrusion north of Nauchas, SWA, the surrounding granites and repeated folding in the younger Damara system*. Unpubl. D.Sc. thesis, Univ. Pretoria, 203 pp.

Dickinson, W.R. 1973. Reconstruction of past arc-trench systems from petrotectonic assemblages in the island arcs of the western Pacific, 569-601. *In*: P.J. Coleman (ed.) *The Western Pacific: Island Arcs, Marginal Sea, and Geochemistry*. Crane and Russak, New York.

Didier, J. 1973. *Granites and their enclaves*. Elsevier, Amsterdam, 393 pp.

Dorais, M.J., Whitney, J.A. and Roden, M.F. 1990. Origin of mafic enclaves in the Dinkey Creek pluton, central Sierra Nevada Batholith, California. *J. Petrol.*, **31**, 853-881.

Govindaraju, K. 1995. Working values with confidence limits for twenty-six CRPG, ANRT and IWG-GIT geostandards. *Geostandards Newsletter*, **19**, 32 pp.

Groote-Biedlingmeier, M. 1974. Tektonik und Metamorphose im Grenzbereich Damara-Praedamara, suedwestlich Windhoek (SWA). *Goett. Arb. Geol. Palaeont.*, **14**, 80 pp.

Heinrichs, H. and Herrmann, A.G. 1990. *Praktikum der analytischen Geochemie*. Springer, Berlin, 669 pp.

Hilken, U. 1998. *Die Altersstellung von metamorphen prae-Damara Plutoniten und Vulkaniten am Suedrand des Damara Orogens (Farm Areb 176, Namibia) abgeleitet aus U/Pb-Isotopenuntersuchungen*. Unpubl. Diplom thesis, Univ. Goettingen, 55 pp.

Kuno, H. 1968. Differentiation of basaltic magmas, 623-688. *In*: Hess H.H. and Poldervaart A. (eds.) *Basalts: The Poldervaart treatise on rocks of basaltic composition*, **2**, Interscience, New York.

Le Maitre R.W. and 11 co-authors. 1989. *A classification of igneous rocks and glossary of terms*. Blackwell, Oxford, 192 pp.

Maillet, P. and 8 co-authors. 1995. Tectonics, magmatism and evolution of the New Hebrides back arc troughs (Southwest Pacific), 176-235. *In*: Taylor (ed.) *Backarc Basins. Tectonics and Magmatism*. Plenum Press, New York.

Maniar, P.D. and Piccoli, P.M. 1989. Tectonic discrimination of granitoids. *Bull. geol. Soc. Am.*, **101**, 635-643.

Master, S. 1990. The “Ubendian” cycle in Equatorial and Southern Africa: Accretionary tectonics and continental growth. *Abstr. 15th Coll. Afr. Geol., CIFEG Occ. Publ.,* **22***, Orleans*.

Master, S. 1993. Early Proterozoic assembly of “Ubendia” (Equatorial and Southern Africa and adjacent parts of Southern America): tectonic and metallogenic implications. *Symp. Early Proterozoic, Geochemical and Structural Constraints-metallogeny. CIFEG Occ. Publ., Dakar*, **23**, 103-107.

Mullen, E.D. 1983. $MnO/TiO_2/P_2O_5$: a minor element discriminant for basaltic rocks of oceanic environments and its implications for petrogenesis. *Earth Planet. Sci. Lett.*, **62**, 53-62.

Nagel, R., Warkus, F., Becker, T. und Hansen, B.T. 1996. U/Pb-Zirkondatierungen der Gaub Valley Formation am Südrand des Damara Orogens/Namibia und ihre Bedeutung für die Entwicklung des Rehoboth Basement Inlier. *Zt. Geol. Wiss.*, **24**, 611-618.

Nesbitt, H.W. and Young, G.M. 1984. Predicition of some weathering trends of plutonic and volcanic rocks based upon thermodynamic and kinetic considerations. *Geochim. Cosmochim. Acta*, **48**, 1523-1534.

Pearce, J.A. and Parkinson, I.J. 1993. Trace element models for mantle melting: applications to volcanic arc petrogenesis, 373-405. *In*: Pritchard H.M., Alabaster T., Harris N.B.W. and Neary C.R. (eds) *Magmatic processes and plate tectonics.* Spec. Publ. geol. Soc. London, **76**.

Pearce, J.A., Harris, N.B.W. and Tindle, A.G. 1984. Trace element discrimination diagrams for the tectonic interpretation of igneous rocks. *J. Petrol.*, **25**, 956-983.

Pfurr, N., Ahrendt, H., Hansen, B.T. and Weber, K. 1991. U-Pb and Rb-Sr isotopic study of granitic gneisses and associated metavolcanic rocks from the Rostock massifs, southern margin of the Damara Orogen: implications for lithostratigraphy of this crustal segment. *Communs geol. Surv. Namibia*, **7**, 35-48.

Reid, D.L., Malling, S. and Allsopp, H.L. 1988. Rb-Sr ages of granitoids in the Rehoboth-Nauchas area SWA / Namibia. *Communs geol. Surv. SWA/Namibia*, **4**, 19-28.

Schalk, K.E.L. 1988. Pre-Damaran basement rocks in the Rehoboth and Southern Windhoek districts (areas 2217D, 2316, 2317A-C) - a regional description. *Unpubl. Rep. geol. Surv. SWA/Namibia*.

Schulze-Hulbe, A. 1979. Pre-Damaran Formations on Marienhof 577, Aroams 315, Doornboom 316 and Göllschau 20, Areas 2316BC and BD, Rehoboth Gebiet. *Unpubl. Rep. geol. Surv. SWA/Namibia*, 45 pp.

Seifert, N. 1986. Geochronologie am Südrand des Damara Orogen, SWA/Namibia: Hydrothermale Beeinflussung von Isotopensystemen und Abkühlalter in präkambrischen Basementgesteinen. *Schweiz. miner. petrogr. Mitt.*, 66, 413-451.

Shand, S.J. 1951. *Eruptive rocks*. J.Wiley, New York, 488 pp.

Stoessel, G.F.U. and Ziegler, U.R.F. 1988. Geochemistry of the Rehoboth basements granitoids, SWA/Namibia. *Communs geol. Surv. Namibia*, **4**, 71-82

Tindle, A.G. 1991. Trace element behaviour in microgranular enclaves from granitic rocks, 313-330. *In*: Didier, J. and Barbarin, B. (eds) *Enclaves and granite petrology*. Developments in Petrology, 13, Elsevier, Amsterdam, 625 pp.

Ziegler, U.R.F. and Stoessel, G.F.U. 1993. Age determinations in the Rehoboth Basement Inlier, Namibia. *Mem. geol. Surv. Namibia*, **14**, 106 pp.